1   # Dynamic Domain Specificity In Human Ventral Temporal Cortex

2   Brett B. Bankson[1,2,4*], Matthew J. Boring[1,3,4], R. Mark Richardson[5,6], Avniel Singh Ghuman[1,2,3,4]

3   [1]Laboratory of Cognitive Neurodynamics, Department of Neurological Surgery, University of

4   Pittsburgh Medical Center, 200 Lothrop Street, Pittsburgh, PA, 15213.

5   [2]Department of Psychology, University of Pittsburgh, 210 South Bouquet St, Pittsburgh, PA

6   15260, USA.

7   [3]Center for Neuroscience at the University of Pittsburgh, University of Pittsburgh, A210 Langley

8   Hall, Pittsburgh, PA 15260, USA.

9   [4]Center for the Neural Basis of Cognition, 4400 Fifth Avenue, Pittsburgh, PA 15213.

10   [5]Department of Neurosurgery, Massachusetts General Hospital, 55 Fruit Street, Boston, MA

11   02144.

12   [6]Harvard Medical School, 25 Shattuck St., Boston, MA 02115.

13

14   Abbreviated title: Temporal dynamics of object individuation

15

16   *Correspondence to:

17   Brett B. Bankson

18   Laboratory of Cognitive Neurodynamics

19   UPMC Presbyterian

20   Suite B-400

21   200 Lothrop Street

22   Pittsburgh, PA 15213

23   bbb17@pitt.edu

24

ABSTRACT

An enduring neuroscientific debate concerns the extent to which neural representation is restricted to networks of patches specialized for particular domains of perceptual input (Kaniwsher et al., 1997; Livingstone et al., 2019), or distributed outside of these patches to broad areas of cortex as well (Haxby et al., 2001; Op de Beeck, 2008). A critical level for this debate is the localization of the neural representation of the identity of individual images, (Spiridon & Kanwisher, 2002) such as individual-level face or written word recognition. To address this debate, intracranial recordings from 489 electrodes throughout ventral temporal cortex across 17 human subjects were used to assess the spatiotemporal dynamics of individual word and face processing within and outside cortical patches strongly selective for these categories of visual information. Individual faces and words were first represented primarily only in strongly selective patches and then represented in both strongly and weakly selective areas approximately 170 milliseconds later. Strongly and weakly selective areas contributed non-redundant information to the representation of individual images. These results can reconcile previous results endorsing disparate poles of the domain specificity debate by highlighting the temporally segregated contributions of different functionally defined cortical areas to individual level representations. Taken together, this work supports a dynamic model of neural representation characterized by successive domain-specific and distributed processing stages.

SIGNIFICANCE STATEMENT

The visual processing system performs dynamic computations to differentiate visually similar forms, such as identifying individual words and faces. Previous models have localized these computations to 1) circumscribed, specialized portions of the brain, or 2) more distributed

1

62   aspects of the brain. The current work combines machine learning analyses with human

63   intracranial recordings to determine the neurodynamics of individual face and word processing in

64   and outside of brain regions selective for these visual categories. The results suggest that

65   individuation involves computations that occur first in primarily highly selective parts of the

66   visual processing system, then later recruits highly and non-highly selective regions. These

67   results mediate between extant models of neural specialization by suggesting a dynamic domain

68   specificity model of visual processing.

69

70   **INTRODUCTION**

71   A key debate regarding the architecture of the cortex concerns the extent to which diagnostic

72   aspects of stimuli are processed within circumscribed, domain-specific and potentially modular

73   cortical networks (Kaniwsher et al., 1997; Martin, 2007; Livingstone et al., 2019), or distributed

74   across large, overlapping sections of cortex as a feature map (Haxby et al., 2001; Op de Beeck,

75   2008). On one hand, an extensive body of primate single unit recordings (Perrett et al., 1984;

76   Tsao et al., 2006), human neuroimaging (Kanwisher et al., 1997; Puce et al., 1996), stimulation

77   (Puce et al., 1999; Hirshorn et al., 2016; Parvizi et al., 2012; Afraz et al., 2006; Pitcher et al.,

78   2007), and lesion studies suggests that perception is causally related to the activity within

79   patches of cortex that respond selectively to preferred stimulus categories (Farah et al., 1995;

80   Schalk et al., 2017). Conversely, the distributed feature map hypothesis is supported by evidence

81   from both neuroimaging and single unit recordings that shows reliable face differentiation

82   outside of strongly face-selective patches (Haxby et al, 2001; Bell et al., 2011) and

83   differentiation of non-face categories within face patches (Kiani et al., 2007; Cukur et al., 2013;

84   Hanson & Schmidt, 2011). This hypothesis posits that category selective patches are clusters that

85   process visual information that is particularly diagnostic for those categories within a larger,

86   continuous feature map that spans ventral temporal cortex (VTC) (Op de Beeck et al., 2008; Mur

87   et al., 2012).

88   Across these hypotheses, a central point of debate concerns the role of activity evoked by

89   stimuli outside of highly selective patches (e.g. face-related activity outside of face patches) and

90   activity evoked by "other" stimuli inside patches selective for particular categories of stimuli

91   (e.g. non-face activity inside face patches). Specifically, a critical tension between the

92   aforementioned hypotheses is whether individual-level discrimination (e.g. recognizing which

93   face or word a person is viewing) can be found outside of putative category-selective patches

94   (Spiridon & Kanwisher, 2002; Nestor et al., 2011). Examining individual level discrimination is

95   crucial because it probes the potential computational role and representational level of activity

96   inside and outside of patches that are highly selective for stimuli at the category level. Indeed,

97   the sparing of category-level discrimination in various agnosias (Damasio et al., 1982)

98   emphasizes that individual representations are a key level in the debate between domain specific

99   and distributed models of processing.

100   To test for the presence of individual-level representations across time in and out of

101   selective patches, the dynamics of face individuation was examined with intracranial

102   electroencephalography (IEEG) in 14 patients with pharmacologically intractable epilepsy. To

103   ensure that face individuation was based on face identity level and not the visual image level, 15

104   different images of each of 14 different identities were used across 5 expressions (anger, sadness,

105   fear, happy, neutral) and 3 gaze directions (left, straight, right). The dynamics of word

106   individuation was examined in 5 additional patients (2 overlapping, 17 total patients in the

107   study). Electrode contacts of interest were restricted anatomically to VTC, inferior to the middle

108   temporal sulcus. Using category localizer data, these contacts were first functionally partitioned

109   into ones that demonstrated high face selectivity (HFS) or high word selectivity (HWS) and

110   those with low face selective (LFS) and low word selective (LWS) responses (Figure 1). Every

111   patient had recordings from both high and low category-selective areas. Once the contacts had

112   been partitioned according to their category selectivity, machine learning analyses (regularized

113   logistic regression) were used to compare the dynamics of individuation within and outside of

114   highly category-selective areas. Above chance classification of individual faces and words was

115   seen in both high and low face and word selective regions, but significant decoding emerged

116   approximately 170 ms earlier in high selectivity regions compared to low selectivity regions.

117   These results suggest a dynamic model of domain specificity in VTC in which processing is first

118   restricted to highly selective regions and then is processed by both high and low selectivity

119   regions.

120

121   **MATERIALS AND METHODS**

122   **Subjects**

123   Experimental protocols were approved by the Institutional Review Board of the University of

124   Pittsburgh and written informed consent was obtained from all subjects. 17 patients (8 female)

125   undergoing surgical treatment for medicine-resistant epilepsy volunteered to participate in this

126   experiment. Patients had previously undergone surgical placement of subdural

127   electrocorticographic contacts or stereoelectroencephalography (collectively referred to as iEEG

128   here) as standard care for clinical monitoring during seizure onset zone localization. The ages of

129   subjects ranged from 20 to 64 years (mean = 39.1, SD = 14.6). None of the subjects showed any

130   ictal events during experimental recording nor epileptic activity on the electrodes used in this

4

131   study. All patients completed a localizer session, 14 patients completed experiment 1, and 5

132   patients (2 overlap) completed experiment 2.

133

134   **Experimental Design: Stimuli**

135   In the localizer session, images of bodies (50% male), faces (50% male), words, hammers,

136   houses and phase scrambled faces were used. Examples of these stimuli are outlined in Figure 2

137   of Ghuman et al. (2014). Phase scrambled images were created in Matlab by taking the two-

138   dimensional spatial Fourier spectrum of the image, extracting the phase, adding random phases,

139   recombining the phase and amplitude, and taking the inverse two-dimensional spatial Fourier

140   spectrum. Each image category was presented 80 times, yielding a total of 480 image

141   presentations. Each image was presented in pseudorandom order and repeated once in each

142   session.

143   For experiment 1, frontal views of 14 different face identities were drawn from the

144   Radboud Faces Database. 15 images of each identity were presented, with 5 expressions (anger,

145   sadness, fear, happy, neutral) and 3 gaze directions (left, right, forward). Each unique image was

146   presented four times, yielding a total of 60 presentations per identity and 840 face image

147   presentations. For experiment 2, 36 different three and four-letter real, pseudo-, false font words

148   were presented 30 times each, yielding a total of 1080 word presentations. Only data from trials

149   corresponding to four-letter real and pseudo-words were considered further for data analysis,

150   corresponding to 16 unique words. Word stimuli were selected to have similar log frequency,

151   mean bigram frequency and bigram frequency by position across similar and dissimilar word

152   pairs (measured using the English Lexicon Project). All stimuli for the three experimental

153   sessions were presented on an LCD computer screen placed ~1 meter from subjects' heads.

154

Experimental Design: Paradigms

156 In all experimental sessions, each image was presented for 900 ms with 900 ms inter-trial

157 interval during which a fixation cross was presented at the center of the screen (~10° × 10° of

158 visual angle for the localizer session and experiment 1, ~6° × 6° visual angle for experiment 2).

159 For the localizer session, images were repeated 20% of the time at random. Subjects were

160 instructed to press a button on a button box when an image was repeated (1-back). Only the first

161 presentations of repeated images were used in the analysis.

162 In experiment 1, subjects completed a gender discrimination task, reporting whether the

163 presented face was male or female via button press on a button box. Each subject completed one

164 or two sessions of the task. All three paradigms were coded in MATLAB (version 2007,

165 Mathworks, Natick, MA) using Psychtoolbox (Brainard, 1997) and custom written code.

166 In experiment 2, subjects completed a lexical decision task, reporting whether the

167 presented word was real or not (pseudoword and false font comparisons) via button press on a

168 button box. Each subject completed one or two sessions of the task. All three paradigms were

169 coded in MATLAB using Psychtoolbox and custom written code.

170

Data preprocessing

172 Electrophysiological activity was recorded at 1000 Hz using iEEG electrodes. Single-trial

173 potential was extracted by band-pass filtering the raw data between 0.2-115 Hz using a fourth-

174 order Butterworth filter to remove slow drift, high-frequency noise, and 60 Hz line noise

175 (additionally using a 55-65 Hz stop-band). For each trial, the power spectrum density (PSD) at 2-

176 100 Hz with a bin size of 2 Hz and time-step size of 10 ms was estimated using a Hann multi-

6

177 taper power spectrum analysis in the FieldTrip toolbox (Oostenveld et al., 2011). For each

178 channel, the neural activity between 50-300 ms prior to stimulus onset was used as baseline, and

179 the PSD at each frequency z-scored based on the mean and variance of baseline activity.

180 Broadband gamma signal was extracted as mean z-scored PSD across 40-100 Hz. Both the single

181 trial potentials (stP) and single trial broadband high-frequency activity (stBHA) were used in all

182 analyses.

183   Trials with a maximum amplitude five standard deviations above the mean across trials

184 were eliminated, as well as trials with a deflection greater than 25 µV between sampling points.

185 These criteria allow the rejection of sampling error or ictal events, and resulted in elimination of

186 less than 1% of trials when applied in this and previous work (Li et al., 2019).

187

188 **Electrode localization**

189 To accurately identify electrode contact location, the co-registration of grid electrodes and

190 electrode strips with cortex was adapted from Hermes et al. (2017). Electrode contacts were

191 segmented from high-resolution post-operative computerized tomography (CT) scans of patients

192 and co-registered with anatomical MRI scans that were conducted before neurosurgery and

193 electrode implantation. This method accounted for shifts in specific electrode location caused by

194 potential deformation of the cortex that arise when utilizing FreeSurfer

195 (https://surfer.nmr.mgh.harvard.edu/, 1999) software reconstructions to co-register with the CT

196 scans. SEEG electrodes were localized with Brainstorm software (Tadel et al., 2011) that co-

197 registers post-operative MRI with pre-operative MRI images. Complete localization

198 (incorporating the following electrode selection step) is depicted in Figure 1. The presence of

199 numerically greater HFS contacts in the left hemisphere than right hemisphere is most likely

200 explained by the larger absolute numbers of left than right hemisphere electrode contacts, a result

201 of electrode placement being guided solely by clinical needs of each patient.

202

203 **Electrode selection**

204 Electrodes were selected according to anatomical and two functional criteria. Anatomically,

205 electrodes of interest were selected from within ventral temporal cortex below the middle

206 temporal gyrus. Specifically, the midline of the middle temporal gyrus was defined as the upper

207 limit for anatomical consideration: the beginning of the middle temporal gyrus was used to

208 define a posterior threshold, and the midline of the middle temporal gyrus terminating at the

209 temporal pole was used as the anterior threshold for electrode selection. We conducted

210 multivariate classification over data from the localizer session to identify face and word sensitive

211 electrodes (described in next section). Functionally, highly category selective electrodes of

212 interest demonstrated a peak six-way face classification d' score greater than 0.8, corresponding

213 to $p < .01$ and a large effect size (Cohen, 1988) for the preferred category (face or word) using a

214 Naïve Bayes classifier. Electrodes were not considered if a d' score greater than 0.8 resulted

215 from systematically lower face or word sTP values relative to other conditions (whereby above

216 chance classification could occur simply by systematically lower response magnitude). Selective

217 electrodes were also required to show a maximal sTP or stBHA response to either faces or words

218 for at least 50 ms during the stimulus presentation period. Within each patient's montage, all

219 VTC electrodes of interest that did not meet the criteria for high selectivity for faces or words

220 were labeled as low selectivity (note that face selective electrodes could be considered low

221 selectivity for words and vice versa). Finally, to control for any systematic differences in

222 anatomic location between high selectivity and low selectivity contacts, the most anterior low

223   selectivity contacts from each montage (which were more numerous and more anteriorly located,

224   in general, than the selective contacts) were removed until the high selectivity and low selectivity

225   contacts from each montage were matched anatomically along the anterior-posterior axis.

226   Functionally, this trimming procedure yielded high selectivity and low selectivity contact

227   populations in each patient's montage with equivalent mean coordinate values along the anterior-

228   posterior axis and ensured that any latency differences between populations could not

229   immediately be attributed to any expected conduction delays. Indeed, recent work has

230   demonstrated a relationship between response onset latency and situation along the anterior-

231   posterior axis, such that more anterior contacts emerged later in time (Schrouff et al., 2020).

232   Note that this anatomical balancing procedure did not meaningfully alter the time course of

233   classification over low selectivity contacts compared to retaining all anterior low selectivity

234   contacts and all results remained similar if non-balanced electrodes were used in the analyses.

235

236   **Multivariate classification: Naïve Bayes classifier**

237   We first used a Naïve Bayes classifier with 3-fold cross validation to examine category

238   selectivity over time at individual electrode contacts throughout ventral temporal cortex. Both

239   sTP and stBHA signal values were used as input features in the classifier with a sliding 100 ms

240   time window (10 ms width) as previous studies have shown increased sensitivity and specificity

241   when using both sTP and stBHA (Miller et al., 2016). Indeed, sTP and stBHA metrics have been

242   shown to capture separate and complementary aspects of the physiology that contribute to visual

243   processing as measured with iEEG (Lescynski et al., 2019). sTP signal was sampled at 1000 Hz

244   and stBHA at 100 Hz, which yielded 110 features (100 mean sTP voltage potentials and 10

245   normalized mean stBHA PSD values). Thus at each time point at each electrode, the classifier

246   was trained on the first 2-folds and performance evaluated on the left out fold for 6-way

247   classification of the six object categories presented in the localizer session. We used the

248   sensitivity index *d'* for face or word category against all other categories to determine face and

249   word selective contacts. *d'* was calculated as Z(true positive rate) – Z(false positive rate), where

250   Z is the inverse of the Gaussian cumulative distribution function.

251

252   **Elastic net regularized logistic regression**

253   To examine the temporal dynamics of face and word individuation, we used elastic net

254   regularized logistic regression with three-fold cross validation implemented with the GLMNET

255   package in Matlab. Elastic net was chosen as a means to identify diagnostic electrode contacts by

256   removing non-informative and/or highly correlated classifier features. These series of

257   classification problems were conducted iteratively in four different electrode populations:

258   individual face classification from experiment 1 data in VTC high face selective contacts and

259   VTC low face selective contacts, and individual word classification from experiment 2 data in

260   VTC high word selective contacts and VTC low word selective contacts. Face identity

261   classification was conducted across expression and gaze direction, effectively varying the low-

262   level visual features of each face identity such that this classification problem was not simply

263   face image classification.

264   sTP signal was first downsampled to 100 Hz to yield an equal amount of sTP and stBHA

265   features. sTP signal was then normalized with a Box-Cox transformation to enhance

266   interpretability of classifier weights. Thus at each time point, sTP and stBHA values from each

267   trial were arranged as a *P*-dimensional vector corresponding to 2 * number of contacts in each of

268   the four predefined electrode contact populations. The time course of face and word

269 individuation was identified by examining the pairwise decoding accuracy of a classifier using 3-

270 fold cross-validation. The regularization parameter (λ) was set a priori to 0.9 to favor more

271 sparse classification solutions. The results of this analysis are depicted in Figure 2. For display

272 purposes, group mean time courses were smoothed with a moving average of 30 millisecond

273 fixed window length.

274   For comparison purposes, L1 regularized logistic regression was also repeated in the

275 same manner as the above elastic net analyses (classification conducted separately for high and

276 low category selectivity populations) to demonstrate minimal difference in the time course of *d'*

277 values from the different regularization procedures. For this analysis, the regularization

278 parameter (λ) was by default set to 1.

279   To demonstrate the robustness of general trends of individuation across high and low

280 selectivity contact populations, the elastic net classification procedure was repeated with

281 additional thresholds determined by dividing face and word contact populations into partitions of

282 equal numbers. To do so, all contacts across all subjects in face and word tasks, respectively,

283 were sorted according to peak d' selectivity value from the category localizer. Then, these

284 contacts were divided into six equal partitions. For example, contacts in the face task were

285 divided into 6 partitions consisting of 71 contacts each. Then, elastic net regularized

286 classification was conducted again according to the following groupings: 1) bottom two

287 partitions labeled as LFS, top four partitions labeled as HFS (corresponding d' value of 0.61

288 dividing the two groups); 2) bottom three partitions labeled as LFS, top three partitions labeled

289 as HFS (corresponding d' value of 0.7 dividing the two groups); 3) bottom four partitions labeled

290 as LFS, top two partitions labeled as HFS (corresponding d' value of 0.82 dividing the two

291 groups). This procedure was repeated for word selective contacts at the following d' thresholds:

292   0.58, 0.67, 0.86. The results of this analysis are depicted in Figure 3. For display purposes, group

293   mean time courses were smoothed with a moving average of 30 millisecond fixed window

294   length. The partitions corresponding to the bottom 1/6 and top 5/6 (and vice versa) are not

295   demonstrated because not all subjects had contacts in the lowest and highest partitions.

296

297   **L1 regularized logistic regression**

298   To examine the diagnosticity of brain activity from high and low category selectivity electrode

299   populations in concert with one another, we repeated the above classification analyses with L1 as

300   opposed to elastic net regularization and examined the proportion of electrode contacts that were

301   entirely penalized and removed from the classifier model. Additionally, all VTC electrode

302   contacts (high and low category selectivity) were used to train each classifier, as opposed to

303   splitting the electrode populations as in the previous analyses. After conducting pairwise face

304   classification and pairwise word classification, the classifier weights from each pairwise

305   classification for each electrode contact were extracted and the number of non-zero (positive or

306   negative) weights for each contact tabulated. The percent of electrode contacts with non-zero

307   weights was determined at every time point after baseline normalization. Baseline normalization

308   consisted of determining the threshold of non-zero weight counts that would yield <1% contacts

309   with non-zero weights during the baseline period. The total percentage of electrode contacts

310   assigned non-zero weights for at least 50 ms across the entire time course was determined, and

311   results from this analysis are depicted in Figure 5A. This change in classifier does not alter the

312   time course of individuation compared to the original elastic net procedure.

313

314   **Electrode Diagnosticity in low category selectivity areas**

12

315 Having examined the contributions of high and low face and word selectivity contacts to

316 exemplar representation, we were then interested in examining whether low face and word

317 selective sites that demonstrated selectivity for a different category differed in their contributions

318 to exemplar representation from low face and word selective sites that did not demonstrate any

319 other category selectivity. The main question here is the extent to which contacts that

320 demonstrate category selectivity will contribute to exemplar representation for a different

321 category. Thus in addition to examining high and low category selective contacts, we further

322 decomposed the low face and word category selective populations into two sub groups: other

323 category selective (OCS) and not category selective (NCS). Category selectivity was established

324 with the same method as outlined above, and weights extracted in the same method as above.

325 The results of this analysis are depicted in Figure 5B and demonstrate that higher (but

326 comparable) proportions of NCS than OCS electrode contacts survive penalization and

327 contribute diagnostic information to exemplar classification using L1 regularization.

328

329 **Electrode diagnosticity as a continuous function of category selectivity**

330 To provide a non-binary depiction of the activity profiles of electrode contacts during face and

331 word individuation, we examined the relationships between the time course of electrode weight

332 magnitude and category selectivity. As a first comparison, peak d' value from the category

333 localizer was compared to the latency of peak weight value for each contact. This comparison

334 was conducted separately for face and word individuation. For clarity, only contacts with peak

335 weight values greater than 1 standard deviation above mean baseline (pre-stimulus) value were

336 included. Weight value in this instance, similar to the previous two paragraphs, refers to the

337 mean weight assigned to each contact for each of the pairwise exemplar comparisons at every

13

338   time point. High and low selectivity contacts (for faces and words, separately) were plotted

339   together to demonstrate the general transition from early onset of non-zero weights of highly

340   selective contacts to later onset of low selectivity contacts. The results of this analysis are

341   depicted in Figure 4.

342

343   **Statistical Analyses**

344   For the category localizer with Naïve Bayes classification, row permutation tests on a subject

345   level were used to establish a d' threshold for category selective contacts. For each subject within

346   each permutation, the condition labels for each trial were randomly shuffled and the same

347   classification procedure as above was used 1000 times for a randomly selected channel in each

348   electrode montage. The peak d' value from each permutation was aggregated into a group-level

349   distribution comprising the null distribution from each permutation for each subject. The d' value

350   corresponding to $p < .01$ was estimated from this histogram and used as a selectivity threshold to

351   determine high and low selectivity contact populations for each subject.

352   For face and word individuation as measured with elastic net regularized logistic

353   regression, row permutation tests were used to establish a significance threshold for

354   classification accuracy for each subject. For each permutation, a classifier model was optimized

355   and test condition labels shuffled to test model predictions on randomized data. This procedure

356   was repeated 1000 times to generate a null distribution. The true classification values and null

357   distributions for each subject were combined into group-level distributions, and the mean true

358   classification value and mean null distribution compared to one another. Classification accuracy

359   was deemed significant at a level of $p < .05$ with FDR correction (Benjamini-Hochberg

360   procedure for dependent tests), with a minimum temporal threshold of 3 contiguous significant

14

361   time points. Thus, although different subjects contributed different numbers of contacts to each

362   classification analysis, all subjects are weighted equally in the group mean depicted in Figure 2.

363   Onset sensitivity was determined by with 3 metrics examining the individual subject-

364   level statistics. For the first method, the same true classification values and null distributions

365   from above were compared on an individual level, and the first time point significant at a level of

366    $p < .05$ with FDR correction (Benjamini-Hochberg procedure for dependent tests) with a

367   minimum temporal threshold of 3 contiguous significant time points was used as the onset

368   marker for each subject. Vectors of onset markers compiled from all subjects were compared

369   between HFS / LFS, and HWS / LWS electrode populations with paired-sample t-tests. Because

370   this method is somewhat sensitive to the magnitude of the response (e.g. higher magnitude will

371   cross the statistical threshold sooner) two other methods for calculating onset that are more

372   robust to magnitude differences were used as well.

373   The second onset determination method was adapted from Schrouff et al. (2020): for each

374   subject, the time course of mean classification values for each classification problem (HFS, LFS,

375   HWS, and LWS) were normalized to peak classification value, and a sliding window with 50 ms

376   bins and 10 ms overlap was implemented. Classification average and standard deviation in the

377   baseline period of -100 to 0 ms was estimated, and the first period with 3 contiguous bins

378   surpassing the baseline threshold was marked as the signal onset for a given subject's

379   classification time course. Vectors of onset markers compiled from all subjects were compared

380   between HFS / LFS, and HWS / LWS electrode populations with paired-sample t-tests. Schrouff

381   et al (2020) show that this method for finding onset times is robust to differences in peak

382   magnitude across comparisons.

15

383   For the third onset determination method, onset sensitivity was measured as the first 3

384   contiguous time points where classification values for each subject were greater than 25% of the

385   peak value. Vectors of onset markers compiled from all subjects were compared between HFS /

386   LFS, and HWS / LWS electrode populations with paired-sample t-tests. While 25% of the peak

387   value is not necessarily a strict measure of "onset," it is independent of peak magnitude and

388   provides a metric of whether any differences in peak time are due to differences in slope or

389   whether there is differences in onset (e.g. earlier peak times could be due to sharper rising slope

390   or earlier onset).

391

RESULTS

Spatiotemporal dynamics of individuation

394   Significant face and word individuation was present in and out of HFS and HWS patches (Figure

395   2), as measured with elastic net regularized logistic regression. Using the first method of onset

396   calculation, the onset of face individuation occurred 190 ms earlier in HFS patches relative to

397   LFS patches ($t(13)= 3.05$, $p = 0.009$) and peaked 200 ms earlier ($t(13) = 2.73$, $p = 0.017$), with a

398   higher peak in HFS than LFS patches ($t(13) = 2.68$, $p = 0.019$). Notably, the difference in the

399   magnitude of the HFS and LFS response is independent of the difference in peak times, though

400   onset times can be affected by magnitude differences. Using two other methods of onset

401   calculation that are more robust to differences in magnitude (Schrouff et al., 2020), above chance

402   face individuation occurred significantly earlier inside (160 ms, 210 ms) than outside (250 ms,

403   325 ms) HFS patches ($t(13) = 3.6$, $p = 0.003$; $t(13) = 3.03$, $p = 0.0096$).

404   Word individuation began 145 ms earlier in HWS patches relative to LWS patches ($t(4) =$

405   3.1, $p = 0.036$) and peaked 250 ms earlier ($t(4) = 3.61$, $p = 0.022$), with a higher peak in HWS

16

406   than LWS patches ($t(4) = 2.802$, $p = 0.048$). Using the two other methods of onset calculation

407   that are more robust to differences in magnitude (Schrouff et al., 2020), above chance face

408   individuation occurred earlier inside (150 ms, 190 ms) than outside (285 ms, 405 ms) HFS

409   patches ($t(4) = 1.77$, $p = 0.15$; $t(4) = 4.31$, $p = 0.01$).

410   HFS and HWS patches maintained significant sensitivity to individual face and word

411   representations respectively throughout visual processing (from 130-840 ms and 160-535 ms

412   respectively, $p<0.05$ corrected for multiple comparisons), suggesting that these regions

413   contribute to both early and late visual processing. LFS and LWS reached significance only later

414   (from 320-800 ms and 285 - 605 ms respectively, $p < 0.05$ corrected for multiple comparisons),

415   suggesting that these regions contribute to late visual processing. For both faces and words, the

416   finding of earlier individuation in high selectivity regions relative to low selectivity regions was

417   robust across a range of criteria for defining "high" and "low" selectivity (Figure 3). The

418   robustness of the result demonstrates that illustrating that the differences in timing were not due

419   to choosing an arbitrary threshold between high and low selectivity. Furthermore, see Figure 4

420   for a more continuous rather than binary examination of the relationship between selectivity and

421   timing.

422   Electrodes were placed based on the clinical needs of the patients and not necessarily

423   optimally placed for sensitivity to visual information, thus relative effect sizes are likely more

424   relevant than absolute effect sizes. Peak effect sizes in LFS and LWS patches were relatively

425   small, but nonetheless more than 1/3 that of the peak effect sizes in HFS and HWS patches. This

426   suggests that activity in LFS and LWS patches contributed meaningfully to the overall

427   representation of individual faces and words, albeit less than HFS and HWS patches.

428

Relative contribution of high and low selectivity patches to individuation

The previous results demonstrate that individuation emerges earlier in high selectivity than low

selectivity patches, but leaves the relative contribution of activity in high and low selectivity

patches to the overall individual-level representation unclear. Specifically, two important

questions are outstanding: 1) Is information in category low selectivity patches unique from

information in high selectivity patches? 2) If low selectivity patches contain unique information

that contributes to individuation, is this information present in patches selective to other

categories or patches that show no measured category selectivity, e.g. do word-selective contacts

contribute diagnostic information to face individuation?

Regarding the first question, it is possible that the later, above-chance individuation

accuracy in low selectivity patches is solely due to activity that is highly correlated with activity

from high category-selective patches. If so, this would suggest the information in the low

selectivity patches does not contribute additional information to face or word individuation at the

whole-brain level. To test this hypothesis, sparse classification using L1-regularization and

identical parameters to earlier elastic net procedure except regularization parameter (λ) was

performed over all ventral temporal contacts to identify the electrode contacts that provided

information for face or word individuation. If activity between any set of contacts is highly

correlated, L1-regularization should force all contacts in that set to have zero weight, except the

one with the largest amount of discriminating information. Thus, if low selectivity contacts

convey redundant information to that in high selectivity contacts, low selectivity contacts should

be penalized and removed from the model, given that individuation was weaker for low

selectivity compared to high selectivity contacts (Figure 2). However, if low selectivity contacts

do contain unique diagnostic information that contributes to individuation, a certain proportion

18

452   of low selectivity contacts should be assigned non-zero weights. Note that choice of

453   regularization method (elastic net vs. L1) does not alter the pattern of reported results above. To

454   address the second question, the above analysis was extended by decomposing the low

455   selectivity contacts into "other category-selective" and "not category-selective" populations. This

456   was done by identifying the LFS and LWS contacts that showed high selectivity for any of the

457   other 5 categories in the localizer and those that did not.

458   For both face and word individuation tasks, the analysis showed that proportions of both

459   high selectivity and low selectivity electrode populations contribute diagnostic information

460   (Figure 5A), though high selectivity patches may contribute more than low selectivity ones.

461   Second, decomposing the low selectivity contacts showed that in the face individuation task,

462   regions highly selective for other categories contribute diagnostic information to overall

463   individuation as well as those that demonstrate low selectivity for all categories (Figure 5B).

464   These findings demonstrate that in the later time period of significant individuation in low

465   selectivity contacts, meaningful information that contributed to above chance individuation is

466   present outside of category-selective areas, distributed even to areas that demonstrate selectivity

467   for a different visual object category.

468

469   **Discussion**

470   The presence of individual-level information in and out of highly category-selective areas at

471   different latencies suggests a "dynamic domain specificity" model of visual processing.

472   Specifically, information from a given visual category is first processed primarily in strongly

473   category-selective patches followed by widespread processing that includes both patches that are

474   strongly and weakly selective for that stimulus category (Shehzad & McCarthy, 2018) The

19

475   cascade of neural activity during visual perception is characterized by an early, potentially

476   obligatory, stage of processing in strongly category-selective patches that may guide and gate

477   information for further processing. Previous studies suggest that this early stage represents a

478   coarse pass of processing only allowing for differentiation of relatively distinct images (Hirshorn

479   et al., 2016; Ghuman et al., 2014; Hegdé, 2008). Approximately 150-200 ms later, information

480   then flows to visual processing patches outside of strongly category-selective patches as well,

481   including into patches that are selective for other visual categories, either through lateral and

482   recurrent connectivity or through top-down feedback. Low selectivity patches contribute unique

483   information to the overall individual-level representation (Figure 5) in the later time period

484   (Figure 2), albeit somewhat less information than highly selective patches. Thus, low selectivity

485   patches may help support later visual processing (Hirshorn et al, 2016; Ghuman et al., 2014; Li

486   et al., 2019) that could contribute to determining subtle distinctions between individual category

487   members or assist with later processes such as viewpoint or position generalization (Freiwald et

488   al., 2010). The contribution of low selectivity patches may be particularly important for

489   perception under challenging conditions, such as occlusion or otherwise degraded conditions. A

490   recent iEEG showed that there was little difference in the dynamics of high and low selectivity

491   regions at the category level and that the category-level information in low selectivity regions

492   was redundant with the information in high selectivity regions (Schrouff et al., 2020). The

493   current results focusing on individual-level representation suggest that highly category-selective

494   patches contribute to the neural representation in both early and later processing stages, and low

495   selectivity patches provide non-redundant information that support later processing stages.

496   Regarding the spread of high selectivity contacts throughout VTC, our findings are comparable

497   to the results of other iEEG studies mapping category selectivity which reveal selective contacts

20

498   located on, lateral, and medial to the fusiform gyrus (Kadipasaoglu et al., 2016; Allison et al.,

499   1999) and are not spatially identical to group-averaged categorical topographies as measured

500   with fMRI.

501   The proposed dynamic domain specificity hypothesis may reconcile apparent

502   contradictions between findings that have been used to support domain-specific and distributed

503   feature map models of visual perception. The profound and frank disturbances to the perception

504   of stimuli from particular categories seen in the presence of lesions or disruptions to highly

505   category-selective patches (Puce et al., 1999; Parvizi et al., 2012; Afraz et al., 2006; Farah et al.,

506   1995; Schalk et al., 2017) may emerge due to the perturbation of early and potentially obligatory

507   activity of these areas during visual processing. The perceptual relevance of later activity in low

508   selectivity patches is supported by the current evidence that these patches contribute unique

509   information to face and word individuation (Figure 5). The time of peak individuation in low

510   selectivity patches occurs when significant individuation is still present in high selectivity

511   patches and is near the time when key higher-level visual processes such as viewpoint

512   generalization (Freiwald et al., 2010) and semantic processing (Clarke et al., 2015) occur.

513   Additionally, single units in the medial temporal lobes show selectivity for individual faces in a

514   similar later time period and it has been suggested that this time period is critical for linking

515   perception and memory (Quian Quiroga, 2012; Mormann et al., 2008). Furthermore, this time

516   window is substantially earlier than behavioral reaction times for comparable individual-level

517   face and word recognition tasks (Haxby et al., 1999; Seidenberg & McClelland, 1989). The later

518   information processing in low selectivity patches would also help explain why category

519   discriminant information is sometimes seen outside of category-selective patches in low

520   temporal resolution measures such as fMRI (Haxby et al., 2001; Ghuman & Martin, 2019). As

21

521   such, low selectivity patches may play a role in some aspects of individuation, even if that role is

522   later and more supportive than the central role of strongly selective patches. Causal evidence is

523   required to test whether activity outside of strongly selective patches contributes to perception;

524   for example, an alternative explanation of later discrimination in these regions is that it could

525   reflect a backpropagating learning signal (Rumelhart et al., 1986) rather than perceptual

526   processing.

527   While the results here are consistent with the primarily low temporal resolution data that

528   have been used to support both domain specific and distributed feature map models of VTC

529   organization, they also help address theoretical aspects of the debate between the models.

530   Specifically, in distributed feature map models the difference between strongly and weakly

531   selective parts of VTC is a difference in the degree to which each contributes to perception of

532   stimuli from a particular category, but these contributions should happen at the same processing

533   stage. These models would predict that strongly and weakly selective regions should each have

534   similar timecourses of processing, varying mostly in how much each contributes to the

535   representation for a particular stimulus class. The result that individual-level representations in

536   highly selective regions onset and peak 145 - 250 ms earlier than in weakly selective regions

537   presents a challenge to current instantiations of distributed feature map models. These

538   differences survive across a range of criteria for selectivity (Figure 3), suggesting there is a

539   qualitative, not graded, difference in the role that highly selective regions play for processing

540   stimuli that those regions are selective for relative to the rest of VTC. Thus, continuous feature

541   map models would need to be modified to accommodate relationships between selectivity and

542   latency of information processing.

543 In the strongest versions of domain specificity models, there is no role for regions of

544 VTC weakly selective for a particular category of image in perceptual processing for that

545 stimulus type. However, the results here suggest that these weakly selective regions do

546 contribute to later visual processing. The dynamic domain specificity hypothesis outlined above

547 is an attempt to modify traditional models of domain specificity by positing a supportive role for

548 weakly selective regions that may support later processes and perhaps aid in perception under

549 challenging perceptual conditions.

550 The dynamic pattern of results was seen for both faces, with circuitry that putatively

551 arises from evolutionary and genetic origins, and words, where reading skill must be acquired

552 fully through experience, suggesting dynamic domain specificity may be a general principle of

553 cortical organization. Taken together, these results may reconcile the tension between domain-

554 specific versus distributed feature map models of visual object processing by providing evidence

555 that domain-specific and distributed processing emerge dynamically at different times during the

556 course of visual perception.

557

558   **Author Contributions:** A.S.G designed the experiment. R.M.R. conducted surgical

559   implantations. B.B.B., M.J.B., R.M.R., and A.S.G. collected experimental data. B.B.B. and

560   M.J.B. analyzed the data. B.B.B. and A.S.G. wrote the manuscript.

561   **Data and materials availability:** All data and code is available upon reasonable request to

562   A.S.G (ghumana@upmc.edu).

563

564

565

566

567

568

569

570

571

572

573

574

575

576

577

578

579

580 **References**

581 Afraz SR, Kiani R, Esteky H (2006) Microstimulation of inferotemporal cortex influences face

582 categorization. Nature 442:692-695.

583 Allison T, Puce A, Spencer DD, McCarthy G (1999) Electrophysiological studies of human face

584 perception. I: Potentials generated in occipitotemporal cortex by face and non-face stimuli. Cereb

585 Cortex 9:415-430.

586 Balota, DA, Yap MJ, Hutchison KA, Cortese MJ, Kessler B. Loftis B, Neely JH, Nelson DL,

587 Simpson GB, Treiman R (2007) The English Lexicon Project. Beh. Res. Methods 39:445–459.

588 Bell, A. H., Malecek, N. J., Morin, E. L., Hadj-Bouziane, F., Tootell, B. H. & Ungerleider, L. G.

589 (2011) Relationship between fMRI-identified regions and neuronal category-selectivity. J.

590 Neurosci. 3:12229 – 12240.

591 Brainard DH (1997) The Psychophysics Toolbox. Spat. Vis. 10:433-436.

592 Clarke A, Devereux BJ, Randall B, Tyler LK (2015) Predicting the time course of individual

593 objects with MEG. Cerebr. Cortex 10:3602 – 3612.

594 Cohen J (1988) Statistical Power Analysis for the Behavioral Sciences, ed. 2. UK: Routledge.

595 Cukur T, Huth AG, Nishimoto S, Gallant JL (2013) Functional subdomains within human FFA.

596 J. Neurosci. 33:16748 – 16766.

597 Dale AM, Fischl B, Sereno MI (1999) Cortical surface-based analysis. I. Segmentation and

598 surface reconstruction. NeuroImage 9:179 – 194.

599 Damasio AR, Damasio H, Van Hoesen GW (1982) Prosopagnosia: anatomic basis and

600 behavioral mechanisms. Neurol. 32:331 – 41.

601 Farah MJ, Levinson KL, Klein KL (1995) Face perception and within-category discrimination in

602 prosopagnosia. Neuropsychologia 33:661-674.

603 Freiwald WA, Tsao DY (2010) Functional compartmentalization and viewpoint generalization

604 within the macaque face-processing system. Science 330:845 – 851.

605 Ghuman AS, Brunet NM, Li Y, Konecky RO, Pyles JA, Walls SA, Destefino V, Wang W,

606 Richardson RM (2014) Dynamic encoding of face information in the human fusiform gyrus. Nat.

607 Comm. 5:5672.

608 Ghuman AS, Martin A (2019) Dynamic neural representations: An inferential challenge for

609 fMRI. Trends Cogn. Sci. 23:534 – 536.

610 Hanson SJ, Schmidt A (2011) High-resolution imaging of the fusiform face area (FFA) using

611 multivariate non-linear classifiers shows diagnosticity for non-face categories. NeuroImage

612 54:1715 – 1734.

613 Haxby JV, Gobbini MI, Furey ML, Ishai A, Schouten JL, Pietrini P (2001) Distributed and

614 overlapping representations of faces and objects in ventral temporal cortex. Science 293:2425-

615 2430.

616 Haxby JV, Ungerleider LG, Clark V, Schouten J, Hoffman E, Martin A (1999) The effect of face

617 inversion on activity in human neural systems for face and object perception. Neuron 22:189 –

618 99.

619 Hegdé J (2008) Time course of visual perception: coarse-to-fine processing and beyond. *Prog.*

620 Neurobiol. 84:405 - 439.

621 Hermes D, Miller KJ, Noordmans HJ, Vansteensel MJ, Ramsey NF (2010) Automated

622 electrocorticographic electrode localization on individually rendered brain surfaces. J. Neurosci.

623 Methods 185:293-298.

624   Hirshorn EA, Li Y, Ward MJ, Richardson RM, Fiez JA, Ghuman AS (2016) Decoding and

625   disrupting left midfusiform gyrus activity during word reading. Proc. Natl. Acad. Sci. USA

626   113:8162 – 8162.

627   Kadipasaoglu CM, Conner CR, Whaley ML, Baboyan VG Tandon N (2016) Category-selectivity

628   in human visual cortex follows cortical topology: A grouped icEEG study. Plos One.

629   Kanwisher N, McDermott J, Chun MM (1997) The fusiform face area: A module in human

630   extrastriate cortex specialized for face perception. J. Neurosci. 17:4302 – 4311.

631   Kiani R, Esteky H, Mirpour K, Tanaka K (2007) Object category structure in response patterns

632   of neuronal population in monkey inferior temporal cortex. J. Neurophysiol. 97:4296 – 4309.

633   Leszczynski M, Barczak A, Kajikawa Y, Ulbert I, Falchier A, Tal I, Haegens S, Melloni L,

634   Knight R, Schroeder C (2019) Dissociation of broadband high-frequency activity and neuronal

635   firing in the neocortex. bioRxiv. https://doi.org/10.1101/531368

636   Li Y, Richardson RM, Ghuman AS (2019) Posterior fusiform and midfusiform contribute to

637   distinct stages of facial expression processing. Cereb. Cortex 186.

638   Livingstone MS, Arcaro MJ, Schade PF (2019) Cortex is cortex: Ubiquitous principles drive

639   face-domain development. Trends Cogn. Sci. 23:3 – 4.

640   Martin A (2007) The representation of object concepts in the brain. Annu. Rev. Psycho. 58:25-

641   45.

642   Miller KJ, Schalk G, Hermes D, Ojemann JG, Rao RP (2016) Spontaneous decoding of the

643   timing and content of human object perception from cortical surface recordings reveals

644   complementary information in the event-related potential and broadband spectral change. PLOS

645   Comput. Biol. 12.

646 Mormann F, Kornblith S, Quian Quiroga R, Kraskov A, Cerf M, Fried I, Koch C (2008) Latency

647 and selectivity of single neurons indicate hierarchical processing in the human medial temporal

648 lobe. J. Neurosci. 28:8865 – 8872.

649 Mur M, Ruff DA, Bodurka J, De Weerd P, Bandettini PA, Kriegeskorte N (2012) Categorical,

650 yet graded – single-image activation profiles of human category-selective cortical regions. J.

651 Neurosci, 32:8649 – 8662.

652 Nestor A, Behrmann M, Plaut DC (2011) Unraveling the distributed neural code of facial

653 identity through spatiotemporal pattern analysis. Proc. Natl. Acad. Sci. USA 108:9998 – 10003.

654 Oostenveld R, Fries P, Maris E, Schoffelen JM (2011) FieldTrip: Open source software for

655 advanced analysis of MEG, EEG, and invasive electrophysiological data. Comput. Intell.

656 Neurosci. 156869.

657 Op de Beeck HP, Haushofer J, Kanwisher N (2008) Interpreting fMRI data: maps, modules and

658 dimensions. Nat. Rev. Neurosci. 9:123-135.

659 Parvizi J, Jacques C, Foster BL, Withoft N, Rangarajan V, Weiner KS,Grill-Spector K (2012)

660 Electrical stimulation of human fusiform face-selective regions distorts face perception. J.

661 Neurosci. 32:14915 – 14920.

662 Perrett DI, Smith PA, Potter DD, Mistlin AJ, Head AS, Milner AD, Jeeves AD (1984) Neurones

663 responsive to faces in the temporal cortex: Studies of functional organization, sensitivity to

664 identity and relation to perception. Hum. Neurobiol. 3:197 – 208.

665 Pitcher D, Walsh V, Yovel G, Duchaine B (2007) TMS evidence for the involvement of the right

666 occipital face area in early face processing. Curr. Biol. 17:1568 – 1573.

667   Puce A, Allison T, Asgari M, Gore JC, McCarthy G (1996) Differential sensitivity of human

668   visual cortex to faces, letterstrings, and textures: A functional magnetic resonance imaging study.

669   J. Neurosci. 16, 5205 - 5215.

670   Puce A, Allison T, McCarthy G (1999) Electrophysiological studies of human face perception.

671   III: Effects of top-down processing on face-specific potentials. Cereb. Cortex 9:445 – 458.

672   Quian Quiroga R (2012) Concept cells: the building blocks of declarative memory functions.

673   Nat. Rev. Neurosci. 13:587 – 597.

674   Rumelhart DE, Hinton GE, Williams RJ (1986) Learning representations by back-propagating

675   errors. Nature 323:533-536.

676   Schalk G, Kapeller C, Guger C, Ogawa H, Hiroshima S, Lafer-Sousa R, Saygin ZM, Kamada K,

677   Kanwisher N (2017) Facephenes and rainbows: Causal evidence for functional and anatomical

678   specificity of face and color processing in the human brain. Proc. Natl. Acad. Sciences 114:

679   12285-12290.

680   Seidenberg MS, McClelland JL (1989) A distributed, developmental model of word recognition

681   and naming. Psychol. Rev. 96:523 - 568.

682   Shehzad Z, McCarthy G (2018) Category representations in the brain are both discretely

683   localized and widely distributed. J. Neurophysiol. 119:2256 – 2264.

684   Spiridon M, Kanwisher N (2002) How distributed is visual category information in human

685   occipito-temporal cortex? An fMRI study. Neuron 35:1157 – 1165.

686   Tadel F, Baillet S, Mosher JC, Pantazis D, Leahy RM (2011) Brainstorm: a user-friendly

687   application for MEG/EEG analysis. Comput. Intell. Neurosci. 8.

688   Tsao DY, Freiwald WA, Tootell RB, Livingstone MS (2006) A cortical region consisting

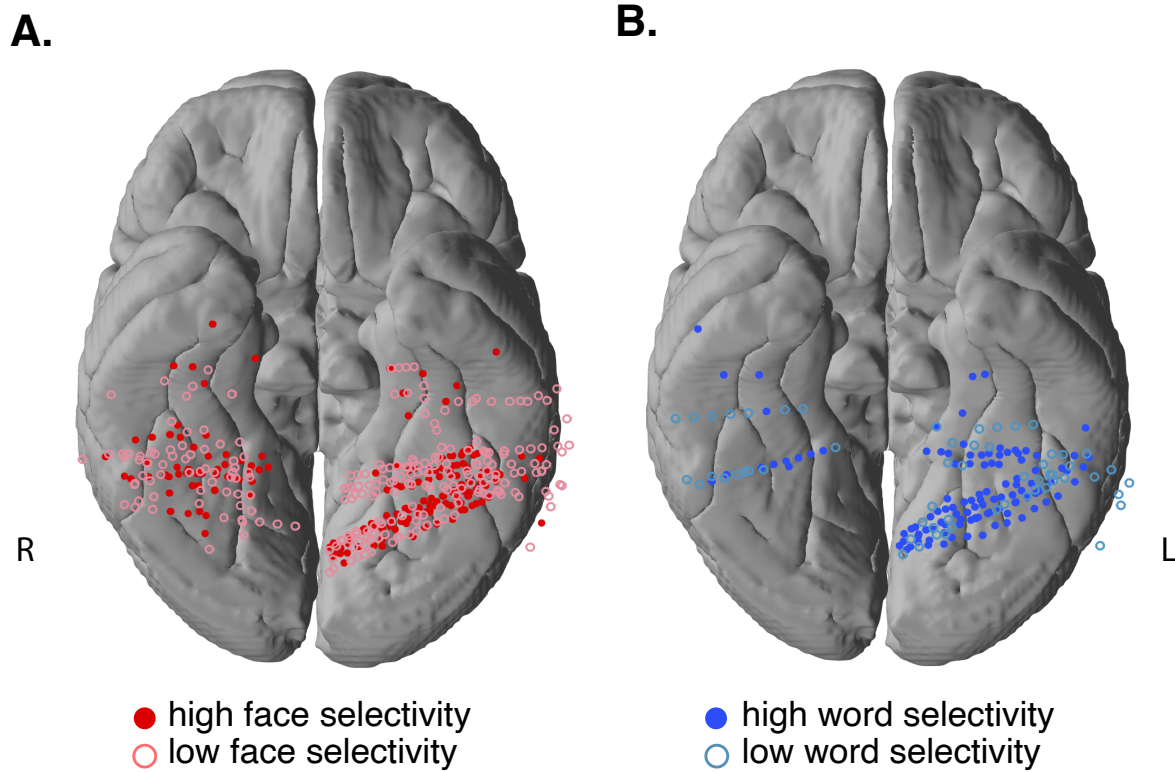689   entirely of face-selective cells. Science 311:670 - 674.

Figure 1. Ventral temporal electrode contacts (489 total). Electrode contacts depicted here include both subdural electrode strips on the surface of the cortex and stereotaxically implanted depth strips, projected to the nearest surface vertex. A) 426 total contacts from 14 subjects were divided into 171 high face selectivity and 255 low face selectivity contacts. B) 174 total contacts from 5 subjects were divided into 113 high word selectivity and 61 low word selectivity contacts.
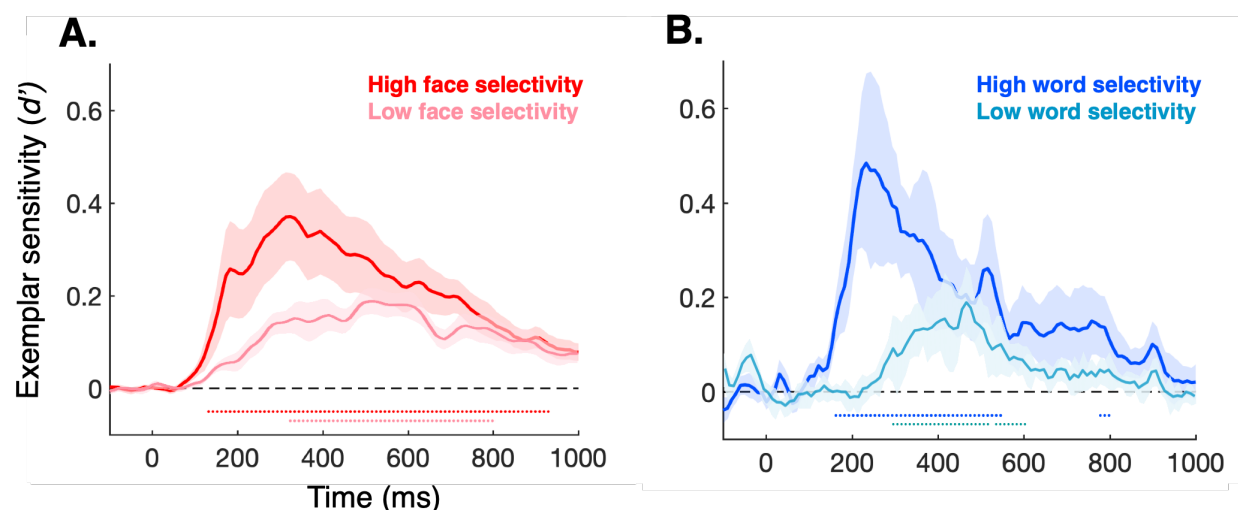
Figure 2. Time course of the sensitivity index (d') for individuation of faces and words. A) HFS contacts (dark red) demonstrated significant face individuation from 130 ms to 840 ms after stimulus onset, with peak $d' = 0.37$ at 320 ms ($p < .05$, FDR corrected for multiple dependent temporal comparisons). LFS contacts (light red) demonstrated significant face individuation from 320 ms to 800 ms after stimulus onset, with peak $d' = 0.17$ at 520 ms ($p < .05$, FDR corrected). HFS individuation onset emerged significantly earlier than LFS individuation (190 ms average difference between HFS and LFS onset, $p = .009$, $t(13) = 3.05$). Individually, 11 of the 14 patients demonstrated an earlier onset of significant individuation in HFS than LFS contacts. B) HWS contacts (dark blue) demonstrated significant word individuation from 160 ms to 535 ms after stimulus onset, with peak $d' = 0.48$ at 235 ms ($p < .05$, FDR corrected for dependent tests). LWS contacts (light blue) demonstrated significant word individuation from 285 ms to 605 ms after stimulus onset, with peak $d' = 0.18$ at 470 ms ($p < .05$, FDR corrected). Word individuation emerged significantly earlier in HWS compared to LWS patches (145 ms average difference between HWS and LWS onset, $p = .036$, $t(4) = 3.1$). Individually, all 5 patients demonstrated an earlier onset of word individuation in HWS compared to LWS contacts. Shaded bars illustrate standard error of the mean across subjects at each time point
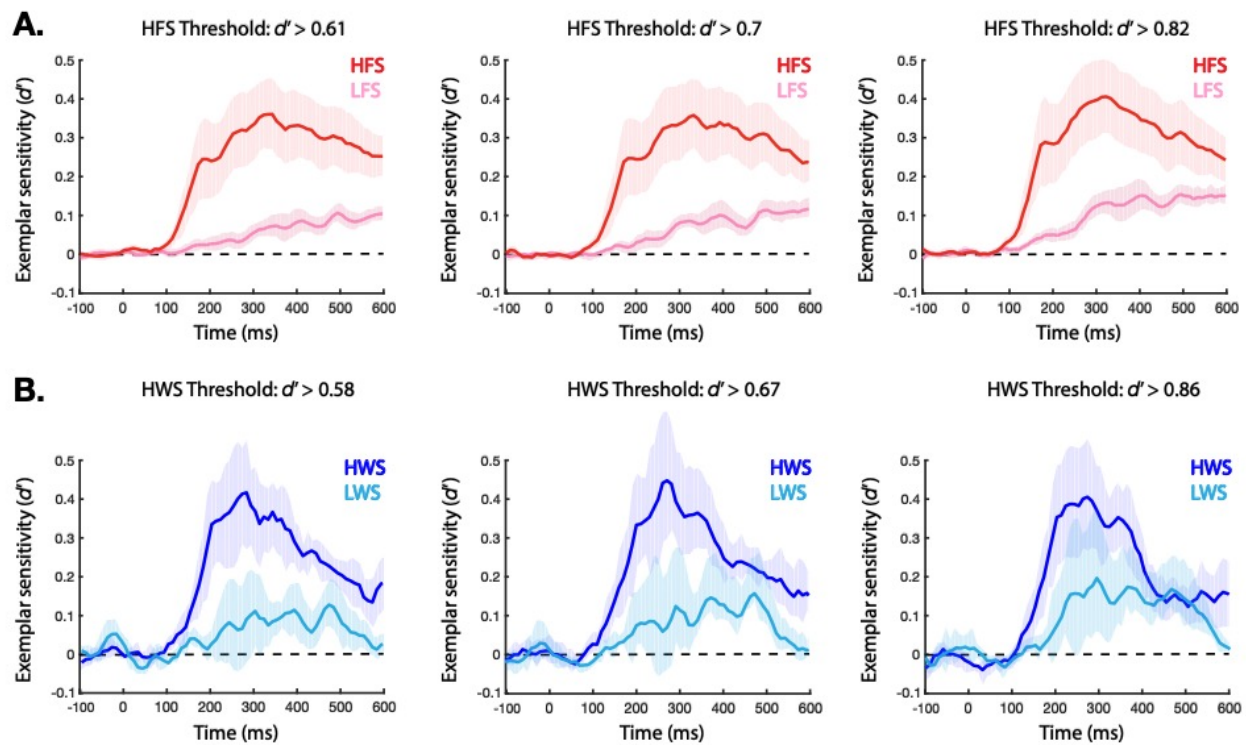
31

Figure 3. Time course of the sensitivity index (*d'*) for individuation of faces and words at graded thresholds. Individual face and word classification (as in Figure 3) was repeated with multiple "high" and low" selectivity thresholds. These thresholds were defined by separating all contacts into partitions corresponding to the one third, one half, and two-thirds levels of d' values as measured with the category localizer. A) Time course of face individuation at thresholds of d' = 0.61 (LFS = bottom 1/3 of contacts, HFS = top 2/3 of contacts), d' = 0.7 (LFS = bottom ½ of contacts, HFS = top ½ of contacts), and d' = 0.82 (LFS = bottom 2/3 of contacts, HFS = top 1/3 of contacts). B) Time course of word individuation at thresholds of d' = 0.58 (LWS = bottom 1/3 of contacts, HWS = top 2/3 of contacts), d' = 0.67 (LWS = bottom ½ of contacts, HWS = top ½ of contacts), and d' = 0.86 (LWS = bottom 2/3 of contacts, HWS = top 1/3 of contacts).
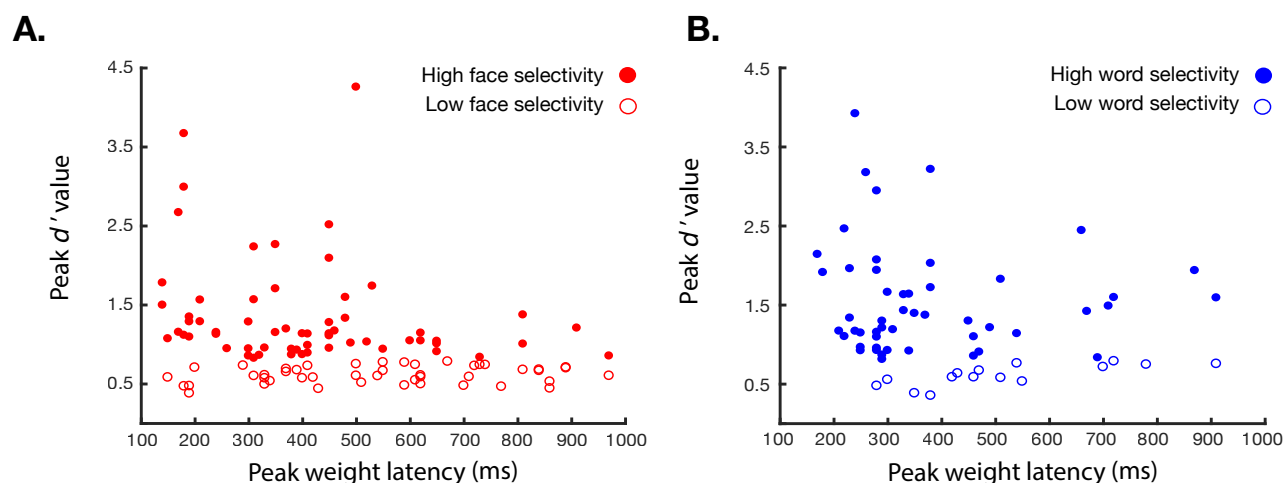
Figure 4. Relationship between selectivity (*d'*) and latency of exemplar information. The selectivity metric was extracted from the category localizer used to define HFS/HWS and LFS/LWS populations. Exemplar information as measured with peak weight value refers to the mean weight assigned to each contact for each of the pairwise exemplar comparisons at every time point for the L1-regularized classifier used for Figure 2. A) Scatter plot depicting latency of peak weight value for HFS and LFS contacts by peak category selectivity value. For this depiction, only contacts with peak values > 1 standard deviation above mean group baseline weight value were included because in electrodes with little diagnostic signals peak times are unreliable and mostly random. 20 out of 62 HFS electrodes have peaks and 6 out of 46 LFS electrodes peak prior to 300 ms. R^2 between *d'* and peak weight latency = 0.11 (p = 0.006). B) Scatter plot depicting latency of peak weight value for HWS and LWS contacts by peak category selectivity value (same thresholding as A). 26 out of 50 HWS electrodes have peaks and 2 out of 15 LWS electrodes peak prior to 300 ms. R^2 between *d'* and peak weight latency = 0.04 (p = 0.11). This set of results shows that both for word and face processing, more selective electrode contacts have earlier peak weight latencies than less selective electrode contacts. These data speak to a relationship between category selectivity and latency of face or word individuation.

739   However, the existence of inter-subject variability and weak correlation means we cannot rule

740   out a graded or binary relationship among electrode contacts based on degree of category

741   selectivity as some correlation would be expected in either case.

742

743

744

745
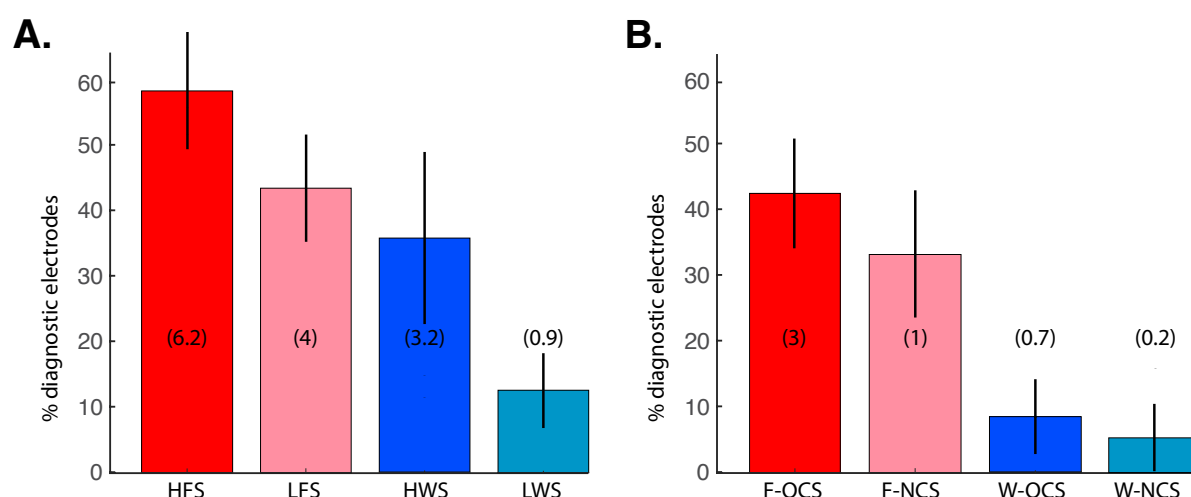
746

747

748

749

750

751

752

753

754

755

Figure 5. A) Percent diagnostic electrode contacts in high category-selectivity and low

selectivity populations measured with L1-regularized logistic regression. 58.6% of HFS contacts

from 14 patients (average of 6.2 contacts per subject, SEM = 9%) were assigned non-zero

weights. 42.4% of LFS contacts (average of 4 contacts, SEM = 8.9%) were assigned non-zero

weights on average. 35.2% of HWS contacts from 5 patients (average of 3.2 contacts, SEM =

18%) on average were assigned non-zero weights. 11.4% of LWS contacts (average of 0.9

contacts, SEM = 6.2%) were assigned non-zero weights. B) Within low face selectivity electrode

contacts that demonstrated selectivity for a different object category (F-OCS, other category-

selective), 42.5% of the contacts (average of 3 contacts per montage, SEM = 8.7% of contacts)

were assigned non-zero weights. Within low face selectivity contacts that demonstrated no

selectivity for any object categories (F-NCS, not category-selective), 33% of the contacts

(average of 1 contact, SEM = 9.6%) on average were assigned non-zero weights. Within low

word selectivity electrode contacts that demonstrated selectivity for a different object category

(W-OCS), 9.4% of the contacts (average of 0.7 contacts, SEM = 8.1%) were assigned non-zero

weights. Within low word selectivity contacts that demonstrated low selectivity for any other

771   object categories (W-NCS), 5% of the contacts (average of 0.2 contacts, SEM 5%) on average

772   were assigned non-zero weights.

773

774

775

776

777

778